QUANTITATIVE AND QUALITATIVE USE OF THERMAL ANALYSIS FOR THE INVESTIGATION OF THE PROPERTIES OF GRANULES DURING FLUID BED MELT GRANULATION

Géza Regdon Jr.[1*] and Yasmine Korteby[1]

[1]*Institute of Pharmaceutical Technology and Regulatory Affairs, University of Szeged, H-6720 Szeged, Eötvös utca 6, Hungary*

* Corresponding author: Dr. habil Géza Regdon jr.

Fax: +36-62-545571, Tel.: +36-62-545576, E-mail: geza.regdon@pharm.u-szeged.hu

Abstract

This study describes a novel approach for the use of thermal analysis to study the aftermath of the fluid bed melt granulation process and to depict the growth mechanism of the granules by quantifying the enthalpies of the granules at every physicochemical change using DSC and their mass loss through TG coupled to MS for a qualitative determination of the composition and amount of the evolved gases for the corresponding fragment ion. The experiments were made in-situ with lactose monohydrate and two viscosity grades of PEG (2000 and 6000) as meltable binders with different contents and size fractions. DSC showed the presence of a beta lactose endotherm peak after the melting of alpha lactose and a proportional increase in its intensity with the increase of the particle size and the content of the binder, which suggested a relation with the agglomeration growth. Interestingly, TG and MS showed a larger reduction in the water content from lactose with the increase in the binder particle size, making it possible to evaluate the dehydration during the melt granulation. Indeed, during the distribution mechanism the low binder particle size and viscosity exposed lactose to a high heat transfer from the fluidizing air. However, a high binder particle size results in lactose immersed in the PEG particles, causing water to be trapped inside the granules and hence a larger reduction in water mass loss indicating the immersion mechanism. Therefore, thermal analysis is a promising tool for granulation growth control.

Keywords: Fluid bed melt granulation, Mass spectrometry, TG/MS, DSC, lactose monohydrate, PEG.

1. Introduction

Hot melt technology is a commonly used robust method in pharmaceutical research as it allows the influence of the bioavailability of drugs and numerous applications such as the preparation of eutectic mixtures [1, 2] and solid dispersions in order to provide time controlled, modified, extended, and targeted drug delivery as well as taste masking of bitter active pharmaceutical ingredients (APIs) [3, 4]. Fluid bed melt granulation (FBMG) is another technique that is gaining popularity in the pharmaceutical industry due to its multiple advantages [5, 6]. It uses a molten binder to agglomerate the pharmaceutical powder particles. Following particle agglomeration and consolidation, the granules are cooled to room temperature and a solid end product with a granular structure is formed [7-10]. For this granulation method, the drying step, which is required after wet granulation, is eliminated, hence the process time and energy requirements are significantly reduced. Since no liquids are used, HMG has the possibility to agglomerate moisture-sensitive materials [11, 12]. Furthermore, melt granulation can be used to develop high-dose formulations with up to 90% of active pharmaceutical ingredient (API) [13, 14]. During melt granulation, the thermal energy involved in the melting of the binding material will be induced by the heat transfer from the conveying fluidizing air to the power bed. The latter will bring about changes in the physicochemical properties of the final product, therefore the determination of the favorable process condition for the desired quality attributes of the granules must be established. For years, thermal analysis techniques were used in research to give an insight into the properties of materials and could advantageously be used in the quality control of drug products [15]. The methods are commonly used in preformulation for the study of polymorphism and for the study of the interactions between the drug substance and the excipients, since these physical interactions can be the basis of dosage form performance [16]. For the routine control of the drug products and raw materials, these methods which are quick, automated and require only a few mg of the samples, are very attractive for routine analysis [15, 17]. In preformulation these techniques are particularly valuable for the construction of phase diagrams [18, 19] and the study of the interactions between the drug substance and the excipients. Polymorphism or hydrate formation may be studied by these techniques in granulation and lyophilization for the development of solid dispersions and even in the dosage form [20, 21].

Differential scanning calorimetry (DSC) is a technique used to investigate the response of materials to heating, such as the melting of a crystalline polymer or glass transition [22]. Also, Thermal gravimetric analysis (TGA) provides information on the continuous mass loss

characteristics of the samples to clarify their behavior at a high temperature region, whereas the combination of thermogravimetry and mass spectrometry (TG-MS) allows obtaining especially qualitative information about the composition of evolved gases during the thermal decomposition of solids [23, 24]. A single scan can give several pieces of qualitative and quantitative information about components in the galenical form [25-27]. While the application of thermal analysis began in research, it is now used for development in the control of processes and product quality. Today, thermal analysis is an essential tool for materials research and development, while quality assurance is now one of the hot topics in thermal analysis [28-31].

This study focuses on the off-line analyzed properties of granules prepared by a FBMG process. The different powder compositions and process conditions will determine the structure, growth and properties of the granules. Our approach describes the evaluation of the characteristic thermal responses of granules through the quantification of the mass loss of granules and their enthalpies at every physicochemical change and through a qualitative determination of the composition of the evolved gases (relative amount and shifts in characteristic peaks). This investigation suggests a relation with the agglomeration growth and demonstrates the use of thermal analysis in designing the optimal conditions for the desired quality attributes of products.

2. Materials and methods

2.1. Materials

Alpha-lactose monohydrate (Ph. Eur.) was used as a model filler with a mean particle size of 100.16 µm. Two low melting point polymers: polyethylene glycol 2000; (PEG 2000) and polyethylene glycol 6000; (PEG 6000), (Fluka, Switzerland) were used as meltable binders. The PEG flakes were finely ground using the planetary ball mill PM 100 (Retsch, Dusseldorf, Germany) at 150 rpm for 30 min and then sieved using laboratory test sieves (Retsch , Germany) into different size fractions (63-125, 125-250, 250-500, 500-710, 710-900, 900-1120 µm).

2.2. Fluid bed melt granulation process

PEG and lactose monohydrate were granulated in a Strea-1 (Niro Aeromatic, Bubendorf, Switzerland) fluid bed chamber. A batch size of 200 g was used. The materials were mixed

for 5 min in a Turbula mixer (Willy A. Bachofen Maschienenfabrik, Basel, Switzerland) to homogenize the physical mixture since there are not enough shear forces in the fluid bed granulator. Then they were inserted and fluidized in the preheated chamber for a period of 10 min and at constant air velocity of 2.5 $m.s^{-1}$. The experiments are summarized in Table 1. The varied factors were the viscosity since PEG 2000 and PEG 6000 have different molecular masses and chain lengths, the meltable binder content ranging from 5% to 20% with a step of 5% W/W and the binder particle size in 5 different size fractions. The size fractions 125-250, 250-500, 500-710, 710-900, 900-1120 µm were used regarding PEG 2000 and the size fractions 63-125, 125-250, 250-500, 500-710, 710-900 regarding PEG 6000. The inlet air temperatures were 90 and 100°C for PEG 2000 and 6000, respectively. The outlet air temperatures were 60°C and 70°C for PEG 2000 and 6000, respectively, since the melting point of PEG 2000 and 6000 are 53°C and 63°C, respectively.

2.3. Differential scanning calorimetry

Differential scanning calorimetry (DSC) measurements were performed with a DSC 821^e (Mettler-Toledo GmbH, Switzerland) instrument on raw materials and the corresponding granules after melt granulation. The samples were heated steadily from 25 to 500°C in a non-hermetically sealed 40 µl aluminum pan. The heating rate was $10°C.min^{-1}$. The mass of the samples was 8±1 mg, the measurements were performed in an Argon atmosphere at a rate of 100 $ml.min^{-1.}$ Three parallel examinations were done for all samples. The curves were evaluated with STARe Software.

2.4. Thermogravimetric analysis–mass spectrometry

The thermal gravimetric analysis (TGA) of the samples was carried out with a Mettler-Toledo TGA/DSC1 instrument (Mettler-Toledo GmbH, Switzerland) in a flowing nitrogen atmosphere (70 $cm^3\ min^{-1}$). Approximately 16 mg of each sample in aluminium pans (100 µl) underwent thermal analysis, with a heating rate of $10°K \cdot min^{-1}$, from 25 to 500°C.

The examination of the granules was supplemented with gas analysis. The TG instrument was coupled to a Thermo Star (Pfeiffer) quadruple mass spectrometer (maximum 300 amu) for gas analysis. The measurements were carried out in nitrogen atmosphere. Ions with various mass numbers were determined with the SEM MID measurement module of the Quadera software. Continuous recordings of sample temperature, sample mass, and heat flow were performed.

The obtained results were exported and then plotted in one coordinate system with the TG curves using the Mettler Toledo Star^{e} software.

3. Results and discussion

3.1. Differential scanning calorimetry

The DSC curves of the raw materials are presented in Figure 1. From the heat flow curve of α-lactose monohydrate three endothermic peaks can be observed. The first endothermic peak corresponds to crystal water evaporation around 142°C. The second peak corresponds to the melting of lactose and has an onset at 217°C and a peak temperature at 222°C, as seen in Table 2. The third peak is a small endothermic peak observed at 245°C, which corresponds to a mass loss step. A small exothermic peak is clearly seen from the DSC curve at 310°C. This peak is the sum of the exothermic degradation and the mass loss endotherm, which occurs in the same temperature region for α -lactose monohydrate [5].

The DSC curve of PEG 2000 exhibited a melting peak at 52°C with an onset at 48°C. On the other hand, PEG 6000 has a melting peak at 63°C with an onset at 57°C due to the difference in the molecular mass of the polymers. From the heat flow curves of raw materials, no glass transition temperature T_g can be identified. This can be explained by the fact that PEG is a crystalline polymer. When the melting point of a crystalline material is reached, the solid state transfers abruptly from the solid to the molten state and makes the PEG binder melt. Therefore, the influence of temperature elevation on the properties of the granules is negligible [4].

In Figure 2, the DSC curves of the granule samples prepared with PEG 2000 and 6000 are presented for different binder contents and a fixed binder particle size. We noticed from the heat flow curves that the melting point of PEG 6000, appearing in all samples, has shifted about 5°C lower than observed in its pure form. A wide range of papers describe that polymeric chains exhibit a different organization and properties (i.e. thermal transition, chain conformation) in the presence of a solid surface (i.e. filler, plasticizer) compared to polymeric chains in the bulk [4]; this is caused by the filler molecules that will get in between the polymer chains, space them out of each other and hence increase the free volume. Molecules can then slide past each other more easily, resulting in a decrease of the melting point. In addition, this mobility becomes more expressed at a higher filler concentration. Indeed, the

heat flow enthalpy of the melting of PEGs depends on binder concentration as can be seen for S15 and S13, where the filler content increased and the melting temperature of the binder decreased, respectively.

On the other hand, the loss of crystal water from α-lactose monohydrate did not appear in the same thermal range as in the raw material (Table 3), attributed to the free volume experienced when in contact with the polymer, lowering the crystal vaporization temperature. Also, the normalized integration of the signal intensity demonstrates a decrease when using a higher binder content [8].

However, the most predominant observation was the presence of an endothermic peak between the melting of α-lactose monohydrate and its decomposition (Fig. 2). The peak had an onset at 225°C and 227°C for PEG 2000 and 6000, respectively, and a peak temperature at 229°C and 227°C for PEG 2000 and 6000, respectively (Table 2). This peak is present only in granulated samples, which suggests that it is a result of the melt granulation process. This reveals important information on granule formation, namely that low viscosity polymer (PEG 2000) in a low content generated this small endotherm peak, while with the increase of content the intensity of the peak increased proportionally.

According to the hypothesis of Mašić et al [12], after the dehydration of lactose monohydrate and the melting of anhydrous α-lactose, recrystallization into β-lactose occurred, followed by the melting of anhydrous β-lactose (which corresponds to the above-mentioned endotherm melting peak). So first it is needed to know that beta lactose is a low hygroscopic material with high storage stability and appropriate for water sensitive drugs formulations, which is one of the key points of FBMG [32]. Figure 3 shows the evolution of the β-lactose melting peak with different binder particle sizes. The intensity of the peak is proportional to the increase of binder content, showing that the presence of PEG influences the conversion of α-lactose monohydrate into anhydrous β-lactose. Indeed, when using a low viscosity and a low binder content and size, the mechanism taking place is the distribution mechanism. The lactose is exposed to the hot fluidizing air and the transformation to β-lactose starts showing. However, the increasing binder particle size and content generate a higher wetting surface for more growth by coalescence. This increase is proportional to the intensity of the peak due to the high heat transfer occurring during the phase change of PEG 2000. On the other hand, the binder particle size had an inversely proportional effect on this endotherm peak (Fig. 3). It can be seen that for granules with a high viscosity polymer 6000 and a high particle size of binder,

the peak height for the melting of lactose is relatively close to the pure filler. Also, the enthalpy of melting β-lactose is less pronounced.

It is clear that the height of the α-lactose melting peak is inversely proportional to the melting peak of β-lactose, which can be explained by the granulation growth during the process. Since in this system the immersion mechanism dominates, the particles of lactose will be immersed inside the PEG particle, which will have a restricted mobility; this will cause the filler to stick to the surface of the polymer and get immersed, shielding it from the fluidizing air temperature and hence from dehydration and will result in the low β-lactose melting peak intensity. This indicates the possibility to determine the relative structure of the granules and their mechanism of formation. It helps validate the results obtained, suggesting the binder particle size as the parameter with the greatest influence on the growth mechanism.

3.1. Thermogravimetric analysis

The burning characteristics of the samples obtained from thermogravimetric analysis (TG-DTG) may be used to effectively compare the decomposition characteristics of the raw materials and their blends in granules. The TG curve of α-lactose monohydrate shows three distinctive stages. The first mass loss of 4.52% is observed between 136 and 160 °C (Table 3).

This mass loss is attributed to the elimination of crystal water as it clearly illustrates that the heating resulted in the loss of 1 mole of bound water and is in agreement with the theoretical value of 1 mole of water in lactose monohydrate (5%) [32]. However, researchers reported that the first and major mass loss of water occurred between 40 and 130 °C and was presumably the loss of surface water [1, 22, 32]. The second mass loss occurred between 222 and 265°C and peaked at 153°C, accompanied by a mass loss of 14.55% caused by the thermal decomposition of lactose monohydrate. This process is called pyrolysis. The primary reaction products of pyrolysis tend to polymerize, resulting in brown and black colored macromolecules. Eventually, lactose becomes black on heating. Another mass loss is observed between 290 and 330°C with a mass loss of 55.68%. This step can be interpreted as being due to the addition of the mass loss of decomposition of water and carbon dioxide. Regarding the TG profile of PEG 2000 and 6000, only one mass loss was observed between 388 and 438 and peaked at 415°C with a mass loss of 98.79%, and it corresponds to the decomposition of the materials. The TG and DTG curves of the raw materials are shown in Fig. 4.

Table 4 shows the temperature ranges, peak temperatures, mass loss and the normalized integral of granule samples. The main characteristics of the samples derived from TG-DTG curves such as reaction regions and corresponding mass loss values were used to define the thermal behavior and combustion characteristics of granules. In these regions, one of the most important thermal reactions is the elimination of water molecules through dehydroxylation. The dehydroxylation temperature can be influenced by the amount of impurities present in the material and the degree of disorder in the granules. Regarding the latter, the amount of lactose is higher than the PEG and the temperatures of dehydroxylation were found to be in relation with the crystallinity of lactose for a lower crystallinity index when increasing the PEG content. Hence the operating parameters during the FBMG will determine the final attributes of the granules, giving an insight into the design space that must be assured for the desirable final product.

It can be seen that mass loss in granules comes in four stages. The first mass loss occurred between 80 and 140°C. This thermal range includes two stages of mass loss. The first dehydration between 80 and 100°C is attributed to the elimination of water molecules adsorbed on the external surfaces of the lactose particles as well as a second stage between 100 and 140°C, corresponding to the loss of crystal water. This theory is based on the known stages of mass loss of lactose monohydrate as well as the presence of the polymer that shifted the mass loss of the granules by 2 to 5°C, which is caused by the increase in the free volume in the granules.

The differences in the thermal range of the first mass loss in granules were due to the granules' structure and composition. The evolution of the second stage is illustrated in Fig. 5.

It describes the evolution of the water content of the granules during the granulation process. The intensity of the mass loss varies with the binder content and with the binder particle size. This variation is linked to the formation of granules. When using a low binder particle size, the growth mechanism taking place is the distribution, the binder in a molten state will spread on the surface of the lactose enabling the formation of nuclei and hence the formation of granules. This growth mechanism gives definite attributes to the structure of granules [12]. The porosity and friability of the granules are increased, making the lactose particles subject to hot fluidizing air and hence to dehydration. The amount of water content in the granules will be described as water release. Indeed, there was a small reduction in mass between 80°C and 131°C for S03 and S13 indicating that the raw material α-lactose monohydrate contained

more surface water than the granule, which leads to the conclusion of the granule growth being in relation with the composition of the granules, determined by the conditions established during the granulation process. The increase in the binder content slightly affected the water content of the granules. Fig. 5 shows that the mass loss slightly increased with the increase in binder content, which can be interpreted as a prevention of mass reduction as it helped shield the lactose particle from the hot fluidizing air. As for the viscosity grade, its influence could be seen when in high grade, as in the case of PEG 6000. Table 4 shows the variation of the four stages of mass loss for both PEG 2000 and 6000 viscosity gradients. The use of a low viscosity grade binder combined with a low binder content and particle size showed a poor mass loss in the first stage, which is attributed to a specific growth mechanism. The distribution of the melted binder over the lactose particles will result in adhesion and formation of nuclei. The latter will agglomerate if enough binding surface is available and will form granules. Their final structure gives the latter defined quality attributes. The lactose particles will be submitted to high temperature during granulation and with the distribution mechanism only a small part of the granules will be covered with the binder PEG 2000.

This result could be quantified with TG. A mass loss in the lactose crystal water was identified. This mass loss was very low compared with the raw material due to the dehydration of crystal water during the heating phase of the melt granulation. The mass loss was proportional to the increasing binder content. The increased binding surface resulted in lactose being covered and a low dehydration process (Table 4). However, the increase in binder viscosity led to a mass loss which was slightly higher but not significant enough for a change in the granulation mechanism. Indeed, the viscosity plays only a secondary role in the growth of the granules. It is the binder particle size that has the primary effect and the results showed that the increase in binder content even at low binder content and viscosity grade resulted in a significant mass loss in the first stage of the decomposition of the granules (Fig. 5).

The curves also revealed a shift in the melting point of the granules (Table 4). Indeed, the presence of the polymer helped increase the free volume and this explains the temperature drop in the first mass loss stage and water will be given out around 80°C. The higher the amount of the polymer, the lower the temperature at which water is given out. The same can be said when increasing the binder content. The free volume is at its highest value and the shift in temperature is more predominant.

3.2. Mass spectrometry

In order to clarify the decomposition mechanism of the granules, the mass loss during each decomposition process should be characterized by the identified evolution components. The interpretation of the mass spectra occurs on the basis of degassing profiles from the molecule ions of water (H_2O^+: m/z = 16, 17, 18) and ethylene glycol (CH_2OH^+: m/z=31, 32) as well as hydrocarbons as CH_4^+ (m/z = 16) and $C_2H_4^+$ (m/z= 28); carbon oxides as CO^+ (m/z=28) and CO_2^+ (m/z= 44); and other molecules ions summarized in Table 5.

The evolution of gas species has been followed in situ by the coupled TG–MS system. The evolution curves of ion-fragments of various gases released are shown as ion current versus time curves. The characterization of water release by means of MS is possible with the molecule ion H_2O^+ (m/z = 18) together with the fragment ion OH^+ (m/z = 17) and O^+ (m/z = 16). Peaks at 125, 250 and 315°C are found in the ion current curve for H_2O^+ (*m*/*z* = 18); corresponding peaks are also found in the ion current curves for OH^+ (m/z = 17) and O^+ *(*m/z = 16). It can be safely concluded that water is given out at about 125, 250 and 315°C from the samples, which is consistent with the mass loss observed from the TG curves. The dehydration takes place in the minor step at around 125°C, which is attributed to the dehydration of lactose monohydrate.

The ion fragment m/z = 16 (O^+) originates mainly from the evolution of both $H_2O^+$and O_2^+. Some change in intensities of the m/z = 44 fragments was observed, probably as an oxidation effect caused by the intense oxygen evolution. Basically, this fragment ion indicates the evolution of CO_2^+. The ion current curves for the evolved gases show for m/z = 44 an increase in concentration at around 250°C, which is attributed to the decomposition of a material. A further increase in the concentration of CO_2 occurs at 415°C, which is assigned to the decomposition of polyethylene glycol (Table 5).

An important increase in the concentration of polyethylene glycol is recorded for m/z=31 and m/z=33 due to the presence of the binder in the granules. The intensity of the peaks is proportional to the amount of PEG present in the composition of the granules, proving the relative correlation between the quantity of PEG and the evolved gases. The comparison of the granules has shown that their thermal decomposition is determined by different factors, such as their structure and composition, and the increase in concentration in the MS curves corresponds precisely to the mass loss in the TG curves.

4. Conclusion

The thermal decomposition of granules made through In situ fluid bed melt granulation has been examined using DSC and TG–MS, which proved to be very useful techniques for the determination of the thermal decomposition and structure of these pharmaceutical drug delivery products. DSC showed that the binder particle size was responsible for the transition from the distribution to the immersion mechanism. This transition was identified by the conversion from α-lactose into β-lactose monohydrate caused by the dehydration of lactose during the FHMG process.

TG–MS have detected and monitored thermally evolved H_2O^+ (m/z = 18), CO_2 (m/z = 44) and polyethylene glycol (m/z = 31, 33). The temperature of the dehydroxylation of the granules is influenced by the free volume depending on the content and the particle size of the polymer. The increase in concentration in the MS curves corresponds precisely to the mass loss in the TG curves. Regarding the growth mechanism, the distribution mechanism occurred when using a low binder particle size and viscosity. The lactose particles will lose a fraction of the adsorbed water during the heating phase of granulation. However, when using a high binder particle size, the lactose particles will be trapped and immersed in the PEG particles, causing the adsorbed water to be trapped inside the granules.

This theory was proven as a larger reduction in water mass loss indicates the immersion mechanism. The morphology and the structure of the granules were observed to be in relation with their mass loss profiles and helped identify the growth mechanisms through the quantitative evaluation of the TG data and the qualitative determination of the evolved gases. This makes thermal analysis a promising technique for granulation growth control by giving a qualitative and quantitative insight into FBMG.

Acknowledgment

The authors would like to thank the Ministry of Higher Education and Scientific Research of Algeria and the Tempus Public Foundation for the Stipendium Hungaricum scholarship provided to Yasmine Korteby for her PhD studies.

References

[1] Szűts A, Sorrenti M, Catenacci L, Bettinetti G, Szabó-Révész P. Investigation of the thermal and structural behavior of diclofenac sodium-sugar ester surfactant systems. J. Therm. Anal. Calorim. 2009; 95:885-890.

[2] Sekiguchi K, Obi N. Studies on absorption of eutectic mixtures. I. A comparison of the behavior of eutectic mixtures of sulfathiazole and that of ordinary sulfathiazole in man. Chem. Pham. Bull. 1961; 9:866-87

[3] Maniruzzaman M, Boateng JS, Snowden MJ, Douroumis D. A Review of Hot-Melt Extrusion: Process Technology to Pharmaceutical Product. ISRN Pharmaceutics. 2012; Article ID 436763, 9 pages, doi:10.5402/2012/436763

[4] Monteyne T, Heeze L, Mortier STFC, Oldörp K, Cardinaels R, Nopens I, Vervaet C, Remon JP, De Beer T. The use of Rheology Combined with Differential Scanning Calorimetry to Elucidate the Granulation Mechanism of an Immiscible Formulation During Continuous Twin-Screw Melt Granulation. Pharm. Res. 2016; 510:271–284.

[5] Roumeli E, Tsiapranta A, Pavlidou E, Vourlias G, Kachrimanis K, Bikiaris D, Chrissafis K, Compatibility study between trandolapril and natural excipients used in solid dosage forms. J. Therm. Anal. Calorim. 2013; 111:2109-2115.

[6] Ansari MA, Stepanek F. Formation of hollow core granules by fluid bed in situ melt granulation: Modelling and experiments. Int. J. Pharm. 2006; 321:108–116.

[7] Kidokoro M, Sasaki K, Haramiishi Y, Matahira N. Effect of Crystallization Behavior of Polyethylene Glycol 6000 on the Properties of Granules Prepared by Fluidized Hot-Melt Granulation (FHMG). Chem. Pham. Bull. 2003; 51-487-493.

[8] Mangwandi C, Zainal NA, JiangTao L, Glocheux Y, Albadarin AB. Investigation of influence of process variables on mechanical strength, size and homogeneity of pharmaceutical granules produced by fluidised hot melt granulation. Powder Technol. 2015; 272:173-180.

[9] Prado HJ, Bonelli PR, Cukierman AL. In situ fluidized hot melt granulation using a novel meltable binder: Effect of formulation variables on granule characteristics and controlled release tablets. Powder Technol. 2014; 264:498-506.

[10] Zhai H, Li S, Andrews G, Jones D, Bell S, Walker G, Nucleation and growth in fluidized hot melt granulation. Powder Technol. 2009; 189:230-237.

[11] Mašić I, Ilić I, Dreu R, Ibrić S, Parojčić J, Đurić Z. An investigation into the effect of formulation variables and process parameters on characteristics of granules obtained by in situ fluidized hot melt granulation. Int. J. Pharm. 2012; 423:202-212.

[12] Mašić I, Ilić I, Dreu R, Ibrić S, Parojčić J, Srčič S. Melt granulation in fluidized bed: a comparative study of spray-on versus in situ procedure. Drug. Dev. Ind. Pharm. 2014; 40:23-32.

[13] Walker GM, Holland CR, Ahmad MMN, Craig DQM. Influence of process parameters on fluidised hot-melt granulation and tablet pressing of pharmaceuticals powders. Chem. Eng. Sci. 2005; 60, 3867-3877.

[14] Mu B, Thompson MR, Sheskey PJ, O'Donnell KP. Hot-melt granulation in a twin-screw extruder. Chem. Eng. Sci. 2012; 81:46-56.

[15] Weatherley S, BO MU, Thompson MR, Sheskey PJ, O'Donnell KP. Hot-Melt Granulation in a Twin Screw Extruder: Effects of Processing on Formulations with Caffeine and Ibuprofen. J. Pharm. Sci. 2013, 102:4330-4336.

[16] Giron D, Goldbronn C. Use of DSC and TG for identification and quantification of the dosage form. J. Therm. Anal. 1997; 48:473-483.

[17] Vasanthavada M, Wang Y, Haefele T, Lakshman JP, Mone M, Tong W, Joshi YM, Serajuddin ATM. Application of Melt Granulation Technology Using Twin-screw Extruder in Development of High-dose Modified-Release Tablet Formulation. J. Pharm. Sci. 2011; 100:1923-1934.

[18] D. Giron, Thermal analysis and calorimetric methods in the characterisation of polymorphs and solvates. Thermochim. Acta. 1995, 248:1.

[19] Ozawa T. Thermal analysis — review and prospect. Thermochimica Acta. 2000; 355:5–42.

[20] Reitz C, Kleinebudde P. Influence of thermal and thermo-mechanical treatment, Comparison of two lipids with respect to their suitability for solid lipid extrusion. J. Therm. Anal. Calorim. 2007; 89:669–673.

[21] Mojumdar SC, Sain M, Prasad RC, Sun L, Venart JES. Selected thermoanalytical methods and their applications from medicine to construction. J. Therm. Anal. Calorim. 2007; 90:653- 662.

[22] Gombás Á, Szabó-Révész P, Kata M, Regdon Jr G, Erős I. Quantitative determination of crystallinity of α-lactose monohydrate by DSC. J. Therm. Anal. Calorim. 2002; 68:503-510.

[23] Jayaraman K, Kok MV, Gokalp I. Combustion properties and kinetics of different biomass samples using TG-MS technique. J. Thermal. Anal. Calorim. 2017; 127:1361–1370.

[24] Wang Z. Li H. Zheng J. TG-MS study on the effect of multi-walled carbon nanotubes and nano-Fe_2O_3 on thermos-oxidative stability of silicone rubber. J. Therm. Anal. Calorim. 2016; 126:733-742.

[25] Li S, Yang C, Li C, Yan S. Synthesis, characterization of new bisphenol-based benzoxazines and the thermal properties of their polymers. J. Therm. Anal. Calorim. 2017; 128, 3:1711–1717.

[26] Zohari N, Abrishami F, Sheibani N. A novel simple correlation for predicting glass transition temperature of energetic azido-ester plasticizers through molecular structures. J. Therm. Anal. Calorim. 2017; 127:2243-2251.

[27] Hotová G, Slovác V. Quantitative TG-MS analysis of evolved gases during the thermal decomposition of carbon containing solids. Thermochimica Acta. 2016; 23-28.

[28] Esfe MH. Designing an artificial neural network using radial basis function (RBF-ANN) to model thermal conductivity of ethylene glycol-water-based TiO2 nanofluids. J. Therm. Anal. Calorim. 2017; 127:2125-2131.

[29] Esfe MH, Rejvani M, Karimpour R, Arani AAA. Estimation of thermal conductivity of ethylene glycol-based nanofluid with hybrid suspensions of SWCNT-AL_2O_3 nanoparticles by correlation and ANN methods using experimental data. J. Therm. Anal. Calorim. 2017. 128:1359–1371.

[30] Kullyakool S, Siriwong K, Noisong P, Danvirutai C. Kinetic triplet evaluation of a complicated dehydration of $(CO_4)_2 8H_2O$ using the deconvolution and the simplified master plots combined with nonlinear regression. J. Therm. Anal. Calorim. 2017. 127:1963-1974.

[31] Çepelioğullar Ö, Mutlu I, Yaman S, Haykiri-Acma H. A study to predict pyrolytic behaviors of refuse-derived fuel (RDF): Artificial neural network application. 2016; 122:84-94.

[32] Raut DM, Allada R, Pavan KV, Deshpande G, Patil D, Patil A, Deshmukh A,. Sakharkar DM, Bodke PS, Mahajan DT. Dehydration of lactose monohydrate: Analytical and physical characterization. Der Pharmacia Lettre, 2011; 3:202-212

List of figures:

Table 1: Factors and process parameters of the granulation experiments.

Model filler	PEG grade	PEG content /%	PEG size /µm	Inlet temperature /°C	Outlet temperature /°C
Lactose monohydrate	2000	5 10 15 20	125 – 250 250 – 500 500 – 710 710 – 900 900 – 1120	90	60
	6000	5 10 15 20	65 – 125 125 – 250 250 – 500 500 – 710 710 – 900	100	70

Table 2: Melting peaks and heat flow data of granules prepared with PEG 2000 and 6000 samples (MR: Melting Range, MP: Melting Peak, PH: Peak Height, 1st E.: First enthalpy of lactose).

Sample	PEG Grade	PEG /%	PEG /µm	MR /°C	MP PEG /°C	1st E. /Jg^{-1}	PH of α-lactose /Jg^{-1}	PH of β-lactose /Jg^{-1}
S01	2000	5	125-250	49.5 – 53.7	51.85	-96.57	3.77	1.04
S02	2000	5	500-710	48.5 – 53.7	52.44	-74.02	2.48	1.35
S03	2000	10	125-250	50.0 – 56.1	53.06	-72.23	1.63	2.13
S04	2000	10	250-500	52.3 – 55.2	51.77	-99.61	1.10	0.80
S05	2000	10	500-710	52.1 – 55.9	52.08	-100.36	1.98	1.65
S06	2000	10	710-900	48.7 – 56.1	52.07	-108.11	1.67	2.28
S07	2000	15	125-250	48.5 – 53.6	51.44	-73.93	2.48	1.35
S08	2000	15	710-900	48.5 – 55.9	51.99	-95.96	1.33	2.16
S09	2000	15	900-1120	48.6 – 55.8	52.29	-97.94	1.25	2.29
S10	6000	5	65-125	56.4 – 61.7	58.85	-122.06	3.06	0.76
S11	6000	5	710-900	63.1 – 67.1	63.14	-101.25	1.22	1.22
S12	6000	10	65-125	60.3 – 62.5	60.08	-102.46	2.43	1.35
S13	6000	10	125-250	56.0 – 62.4	60.08	-83.80	2.38	0.99
S14	6000	10	250-500	61.1 – 64.5	60.22	-72.72	3.91	5.32
S15	6000	20	125-250	63.5 – 68.3	63.53	-104.54	1.11	1.16
S16	6000	20	710-900	57.9 – 67.0	63.86	-75.91	1.32	1.10

Table 3: decomposition behavior of raw materials (lactose monohydrate, PEG 2000, PEG 6000).

TG-DTG data		Lactose monohydrate	PEG 2000	PEG 6000
First phase	Thermal range /°C	132 - 155	388 - 439	389 - 438
	Mass loss /%	3.99	103.29	101.03
	Normalized integral /sC^{-1}	-0.21	-	-5.58
	Peak /°C	143.02	53.80	63.24
	Peak height /°C^{-1}	2.35e-03	31.52e-03	29.33e-03
Second phase	Thermal range /°C	228 - 262	-	-
	Mass loss /%	14.55	-	-
	Normalized integral /sC^{-1}	-0.18	-	-
	Peak /°C	241.17	-	-
	Peak height /°C^{-1}	1.94e-03	-	-
Third phase	Thermal range /°C	287 - 328	-	-
	Mass loss /%	55.68	-	-
	Normalized integral /sC^{-1}	-2.44	-	-
	Peak /°C	302.91		
	Peak height /°C^{-1}	15.75e-03	-	-

Table 4: Decomposition behavior of granules prepared with PEG 2000 and PEG 6000 with different binder contents and binder particle sizes (Thermal range: TR, Mass loss: ML, Normalized integral: NI).

Sample	First decomposition phase				Second decomposition phase				Third decomposition phase				Fourth decomposition phase			
	TR /°C	ML /%	NI /sC^{-1}	Peak /°C	TR /°C	ML /%	NI /sC^{-1}	Peak /°C	TR /°C	ML/%	NI /sC^{-1}	Peak /°C	TR /°C	ML /%	NI /sC^{-1}	Peak /°C
S01	89 – 130	2.75	-0.19	114.58	225 – 265	8.06	-0.31	243.45	284 – 332	39.11	-1.59	312.74	366 - 422	9.97	-0.21	398.80
S03	95 – 132	3.43	-0.19	116.54	229 – 266	9.57	-0.29	244.67	285 – 330	33.92	-1.21	310.63	376 – 426	21.08	-0.55	407.98
S04	95 – 132	2.89	-0.20	116.54	229 – 266	8.30	-0.30	244.67	285 - 330	31.10	-1.20	310.63	376 – 429	15.16	-0.59	407.98
S05	98 – 134	3.04	-0.20	118.94	229 - 264	8.69	-0.29	245.02	285 – 331	31.72	-1.26	311.72	377 – 428	16.41	-0.66	408.53
S06	96 – 134	3.61	-0.20	119.46	231 – 265	14.37	-0.27	246.21	285 – 330	30.61	-1.19	311.00	377 – 428	25.04	-0.82	408.02
S07	87 - 129	2.05	-0.14	112.05	230 - 265	7.91	-0.27	245.08	283 – 333	31.85	-1.27	312.65	378 – 429	15.16	-0.83	409.09
S08	97 – 133	3.05	-0.17	118	232 – 266	3.98	-0.26	245.81	307 – 328	26.59	-1.11	307.98	378 – 429	23.42	-0.86	408.28
S09	97 – 133	3.15	-0.18	118	232 – 264	6.08	-0.27	245.95	283 – 328	27.21	-1.12	308.60	379 – 430	24.79	-0.91	409.70
S10	99 - 136	3.36	-0.18	121.43	229 - 265	12.67	-0.31	244.04	286 - 331	36.35	-1.30	311.74	381 - 430	23.72	-0.77	409.00
S11	98 – 136	3.43	-0.19	121.07	228 – 261	10.83	-0.23	242.54	283 – 331	34.26	-1.42	311.20	379 – 428	24.98	-0.51	407.55
S12	96 – 136	3.43	-0.19	120.30	229 – 265	9.96	-0.24	243.73	284 – 330	35.70	-1.45	310.88	380 – 428	16.07	-0.64	408.11
S14	100 – 137	3.67	-0.21	121.76	226 – 266	10.51	-0.25	244.89	284 – 333	27.80	-1.02	312.58	382 – 430	26.77	-1.28	407.68
S15	97 – 135	3.48	-0.18	120.15	226 – 264	5.95	-0.28	243.68	285 – 333	32.01	-1.35	313.11	388 – 424	16.76	-0.30	406.76
S16	101 – 138	2.97	-0.16	123.88	225 – 265	5.04	-0.28	242.69	286 – 331	26.57	-1.10	312.06	385 – 430	25.61	-1.06	409.77

Table 5: Characteristics of evolved gases and their respective thermal range and peak intensity for granules prepared with different binder viscosity grades, contents and particle sizes. (Peak intensity: PI, Thermal Range: TR), T_1, T_2, T_3 are peaks of temperatures of the first, second and third gas evolution, respectively.

Samples	Masse *m/z*	12	16	17	18	22	25	26	27	31	33	39	43	44	45
	TR /°C	279 - 430	283 - 428	234 - 353	97 - 347	271 - 408	378 - 435	377 - 439	294 - 444	296 - 461	389 - 427	234 - 438	233 - 432	237 - 334	273 - 448
	PI /A	4.19E-10	3.45E-09	2.39E-08	9.38E-08	7.00E-11	3.26E-10	1.73E-09	1.89E-08	6.23E-11	9.45E-12	3.15E-11	1.86E-10	1.00E-09	7.17E-11
	T_1 /°C	314	311	124	125	314	403	408	326	312	403	260	315	258	312
S11	PI /A	3.55E-10	2.86E-09	2.35E-08	9.32E-08	3.81E-11	-	-	1.94E-08	4.02E-10	-	1.20E-10	4.51E-10	4.94E-09	2.14E-10
	T_2 /°C	405	414	250	251	380	-	-	411	406	-	310	407	312	406
	PI /A	-	3.44E-09	2.62E-08	1.04E-07	-	-	-	-	-	-	1.21E-10	-	-	-
	T_3 /°C	-	315	314	314	-	-	-	-	-	-	409	-	-	-
	T.R. /°C	274 - 465	101 - 362	95 - 365	93 - 353	274 - 395	359 - 449	376 - 451	290 - 475	293 - 463	384 - 423	208 - 440	284 - 475	235 - 337	276 - 451
	PI /A	3.56E-10	2.34E-09	1.74E-08	6.88E-08	5.82E-11	2.57E-10	1.41E-09	1.61E-08	5.39E-11	7.79E-12	9.13E-11	1.36E-10	1.46E-09	7.01E-11
	T_1 /°C	310	124	125	125	317	416	409	322	312	401	313	314	263	314
S16	PI /A	2.76E-10	2.26E-09	1.82E-08	7.19E-08	3.53E-11	-	-	1.64E-08	2.29E-10	-	8.32E-11	2.91E-10	4.76E-09	1.25E-10
	T_2 /°C	409	249	246	244	357	-	-	393	411	-	403	407	311	403
	PI /A	-	2.84E-09	2.10E-08	8.34E-08	-	-	-	-	-	-	-	-	-	-
	T_3 /°C	-	312	310	313	-	-	-	-	-	-	-	-	-	-
	TR /°C	277 - 469	105 - 427	99 - 335	99 - 353	283 - 335	377 - 437	374 - 444	299 - 469	195 - 454	379 - 430	287 - 442	255 - 424	265 - 336	285 - 338
	PI /A	3.04E-10	1.40E-09	1.15E-08	4.45E-08	4.17E-11	2.28E-10	1.26E-09	1.46E-08	2.74E-11	6.49E-12	8.68E-11	1.22E-10	1.48E-09	6.03E-11
	T_1 /°C	312	122	120	117	292	410	413	336	249	406	311	313	266	312
S12	PI /A	2.54E-10	2.08E-09	1.32E-08	5.22E-08	5.53E-11	-	-	1.51E-08	3.69E-11	-	8.79E-11	3.12E-10	4.23E-09	1.51E-10
	T_2 /°C	404	310	250	249	313	-	-	413	311	-	404	408	311	405
	PI /A	-	1.64E-09	1.57E-08	6.24E-08	-	-	-	-	2.66E-10	-	-	-	-	-
	T_3 /°C	-	415	312	312	-	-	-	-	405	-	-	-	-	-
	TR /°C	282 - 451	104 - 336	92 - 380	100 - 367	287 - 409	368 - 445	302 - 444	266 - 435	222 - 453	382 - 427	213 - 430	271 - 424	228 - 348	
	PI /A	2.14E-10	1.61E-09	1.31E-08	5.06E-08	3.45E-11	2.64E-10	1.17E-09	1.53E-08	2.55E-11	7.52E-12	1.88E-11	7.98E-11	5.55E-10	3.48E-11
	T_1 /°C	315	121	121	118	314	409	318	356	246	405	258	314	257	316
S14	PI /A	2.36E10	1.65E-09	1.37E-08	5.33E-08	2.10E-11	-	1.41E-09	1.58E-08	3.10E-11	-	5.09E-11	3.60E-10	2.19E-09	2.03E-10
	T_2 /°C	404	258	248	248	368	-	406	410	314	-	314	404	316	406
	PI /A	-	1.86E-09	1.43E-08	5.59E-08	-	-	-	-	3.61E-10	-	8.94E-11	-	-	-
	T_3 /°C	-	315	313	313	-	-	-	-	405	-	405	-	-	-

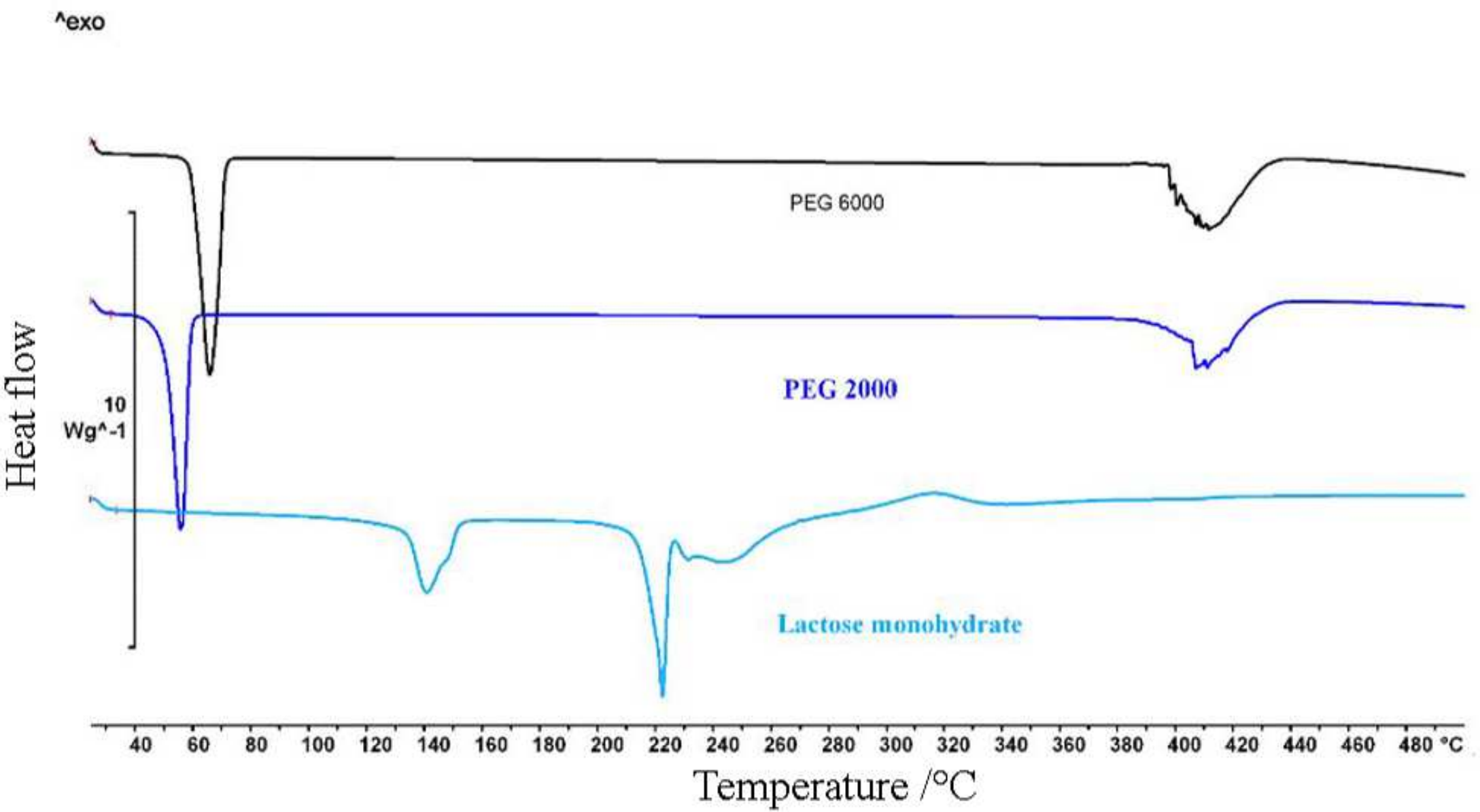
^exo
PEG 6000
PEG 2000
Lactose monohydrate
10
Wg^-1
Heat flow
40 60 80 100 120 140 160 180 200 220 240 260 280 300 320 340 360 380 400 420 440 460 480 °C
Temperature /°C

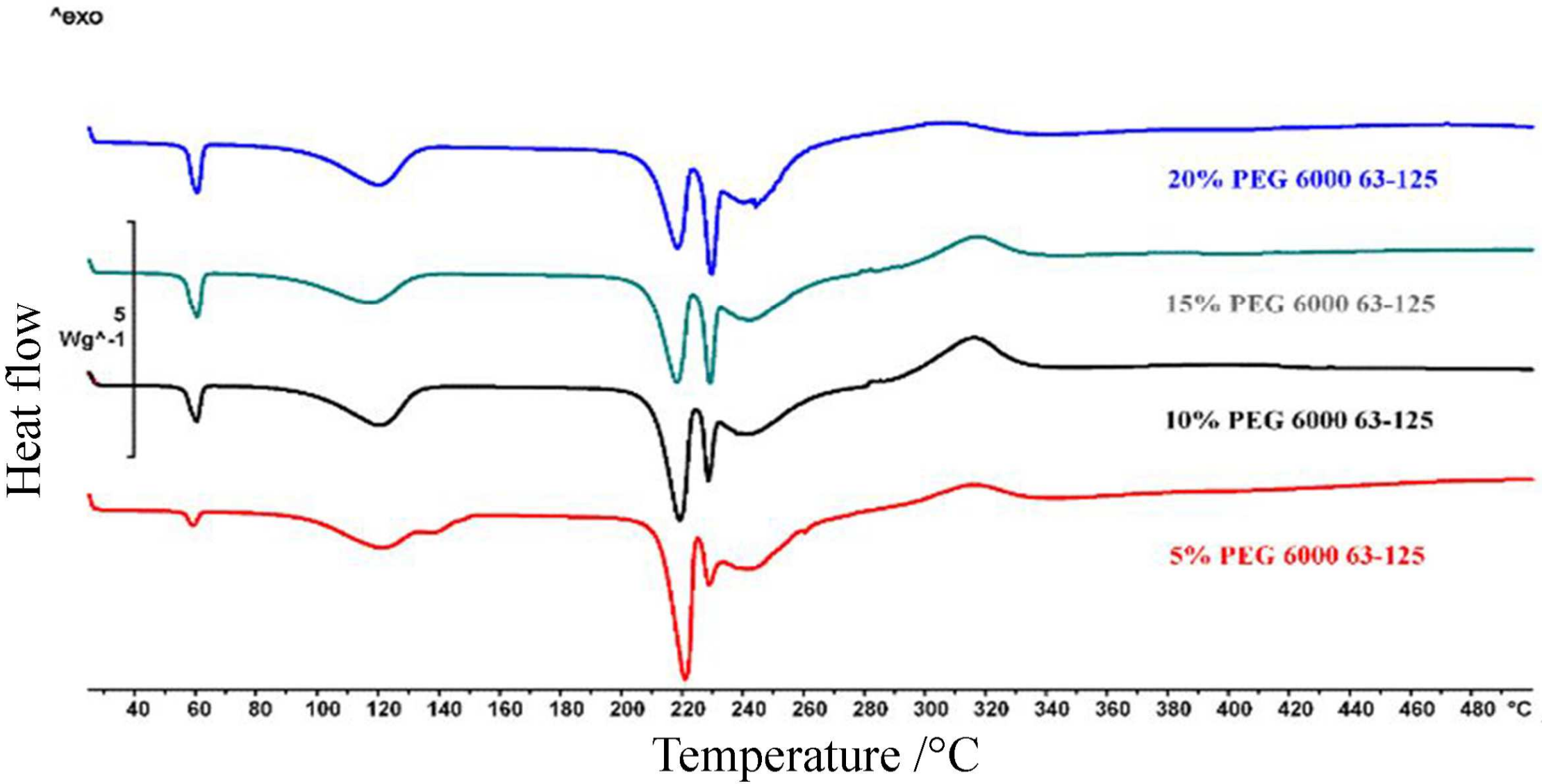
^exo
20% PEG 6000 63-125
15% PEG 6000 63-125
10% PEG 6000 63-125
5% PEG 6000 63-125
5
Wg^-1
Heat flow
40 60 80 100 120 140 160 180 200 220 240 260 280 300 320 340 360 380 400 420 440 460 480 °C
Temperature /°C

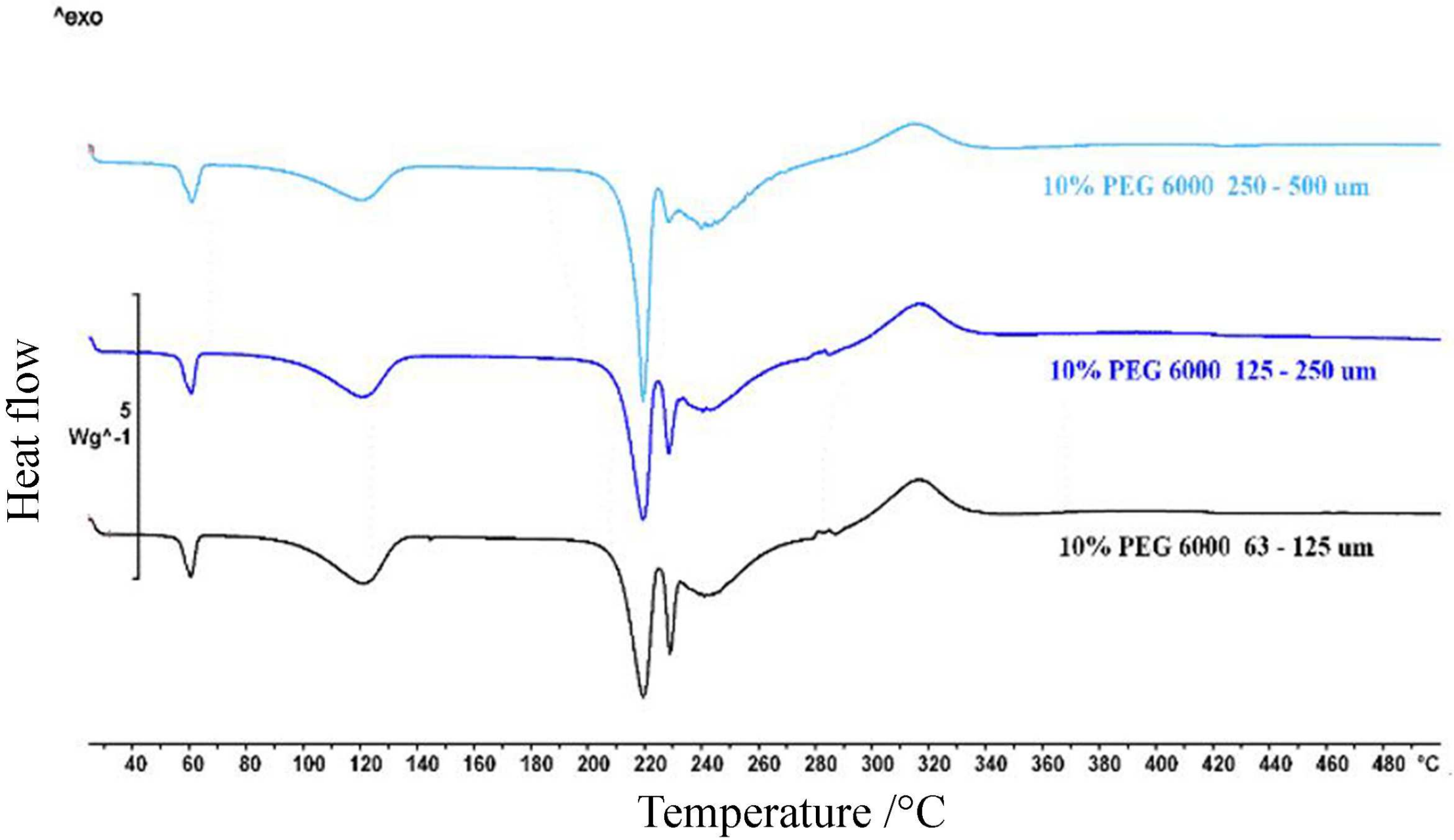
^exo
10% PEG 6000 250 - 500 um
10% PEG 6000 125 - 250 um
10% PEG 6000 63 - 125 um
5
Wg^-1
Heat flow
40 60 80 100 120 140 160 180 200 220 240 260 280 300 320 340 360 380 400 420 440 460 480 °C
Temperature /°C

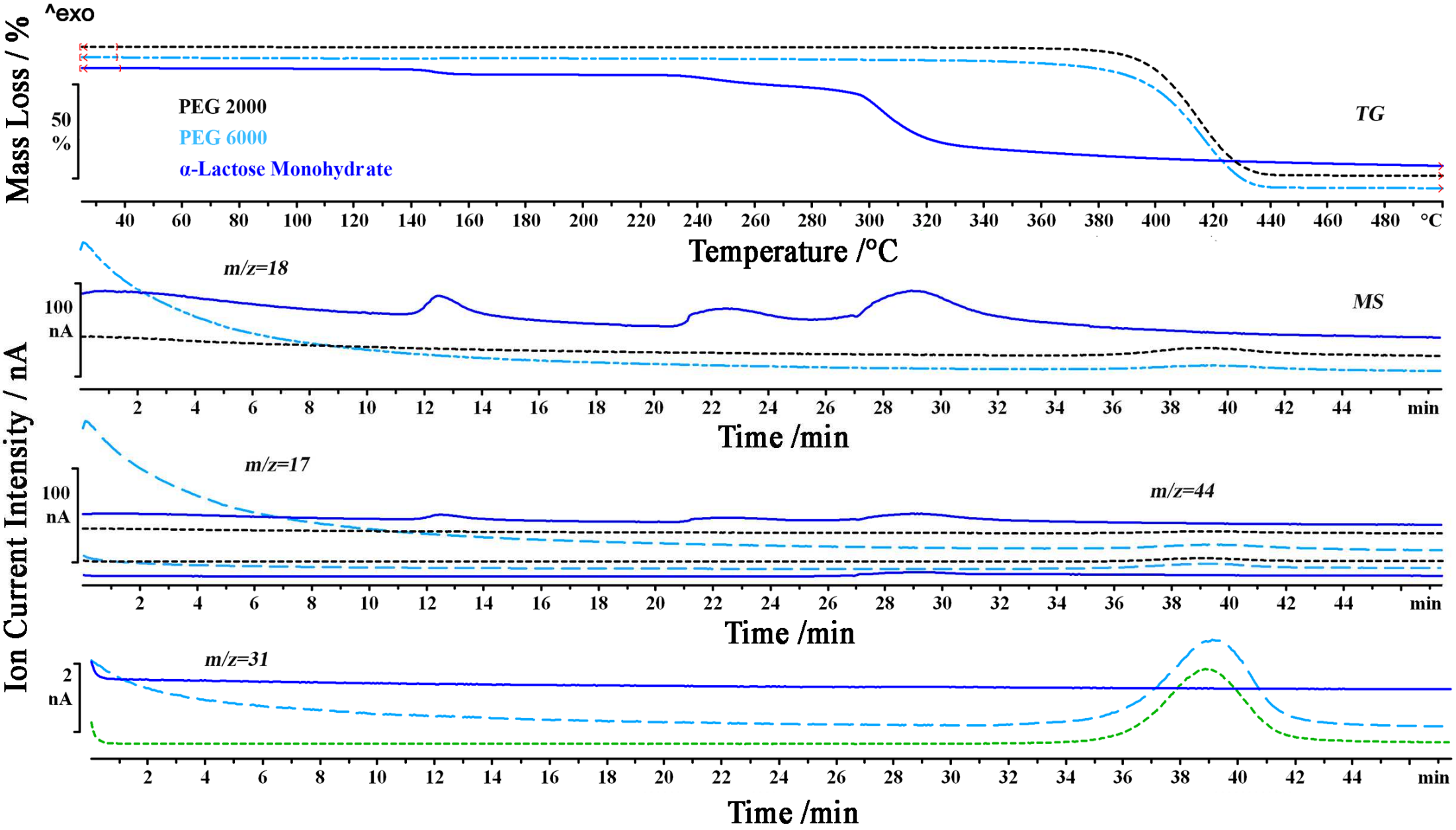
^exo
Mass Loss / %
50
%
PEG 2000
PEG 6000
α-Lactose Monohydrate
TG
40 60 80 100 120 140 160 180 200 220 240 260 280 300 320 340 360 380 400 420 440 460 480 °C
Temperature /°C
Ion Current Intensity / nA
m/z=18
100
nA
MS
2 4 6 8 10 12 14 16 18 20 22 24 26 28 30 32 34 36 38 40 42 44 min
Time /min
m/z=17
100
nA
m/z=44
2 4 6 8 10 12 14 16 18 20 22 24 26 28 30 32 34 36 38 40 42 44 min
Time /min
m/z=31
2
nA
2 4 6 8 10 12 14 16 18 20 22 24 26 28 30 32 34 36 38 40 42 44 min
Time /min

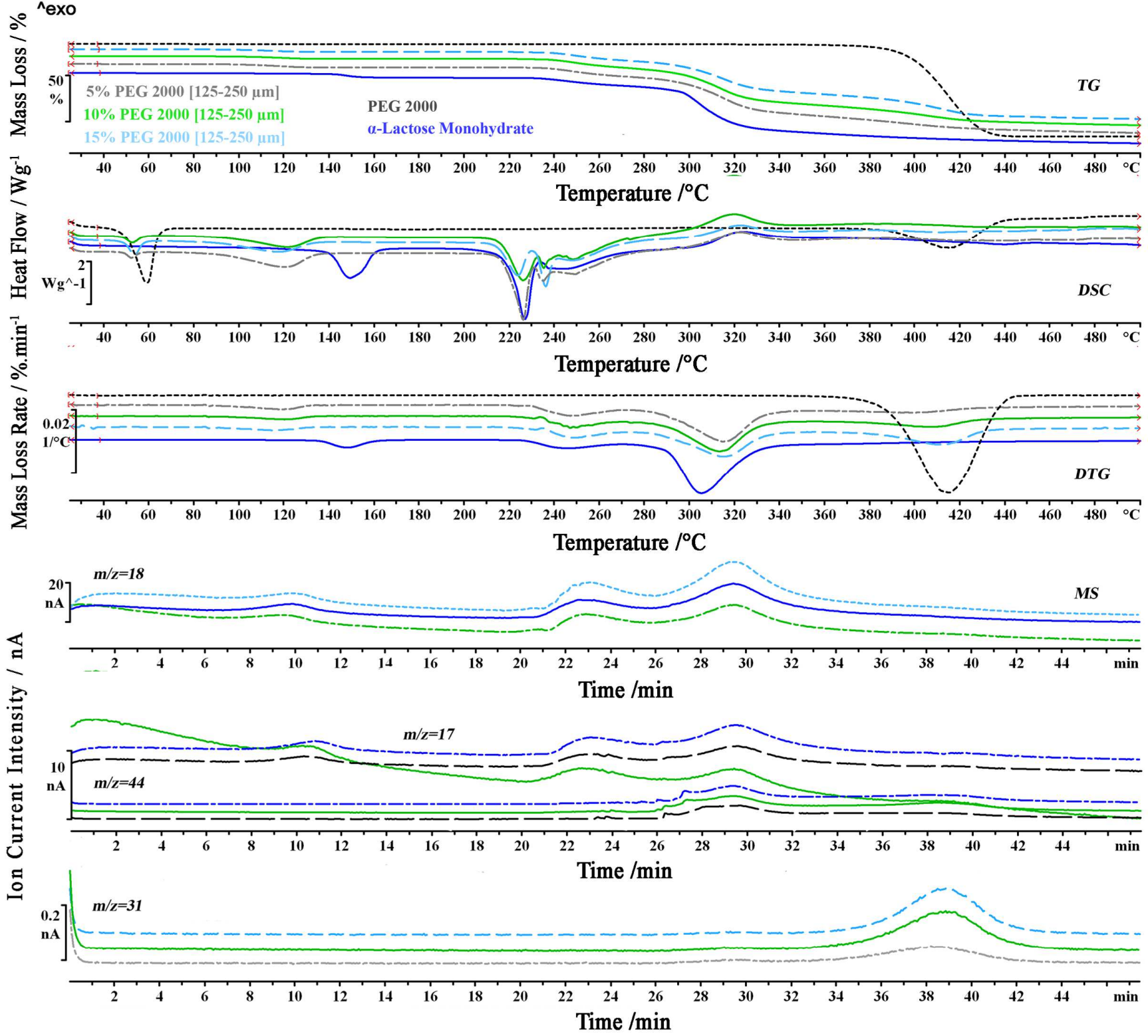
^exo
Mass Loss / %
50
%
5% PEG 2000 [125-250 µm]
10% PEG 2000 [125-250 µm]
15% PEG 2000 [125-250 µm]
PEG 2000
α-Lactose Monohydrate
TG
40 60 80 100 120 140 160 180 200 220 240 260 280 300 320 340 360 380 400 420 440 460 480 °C
Temperature /°C
Heat Flow / Wg-1
2
Wg^-1
DSC
40 60 80 100 120 140 160 180 200 220 240 260 280 300 320 340 360 380 400 420 440 460 480 °C
Temperature /°C
Mass Loss Rate / %.min-1
0.02
1/°C
DTG
40 60 80 100 120 140 160 180 200 220 240 260 280 300 320 340 360 380 400 420 440 460 480 °C
Temperature /°C
Ion Current Intensity / nA
m/z=18
20
nA
MS
2 4 6 8 10 12 14 16 18 20 22 24 26 28 30 32 34 36 38 40 42 44 min
Time /min
m/z=17
10
nA
m/z=44
2 4 6 8 10 12 14 16 18 20 22 24 26 28 30 32 34 36 38 40 42 44 min
Time /min
m/z=31
0.2
nA
2 4 6 8 10 12 14 16 18 20 22 24 26 28 30 32 34 36 38 40 42 44 min
Time /min

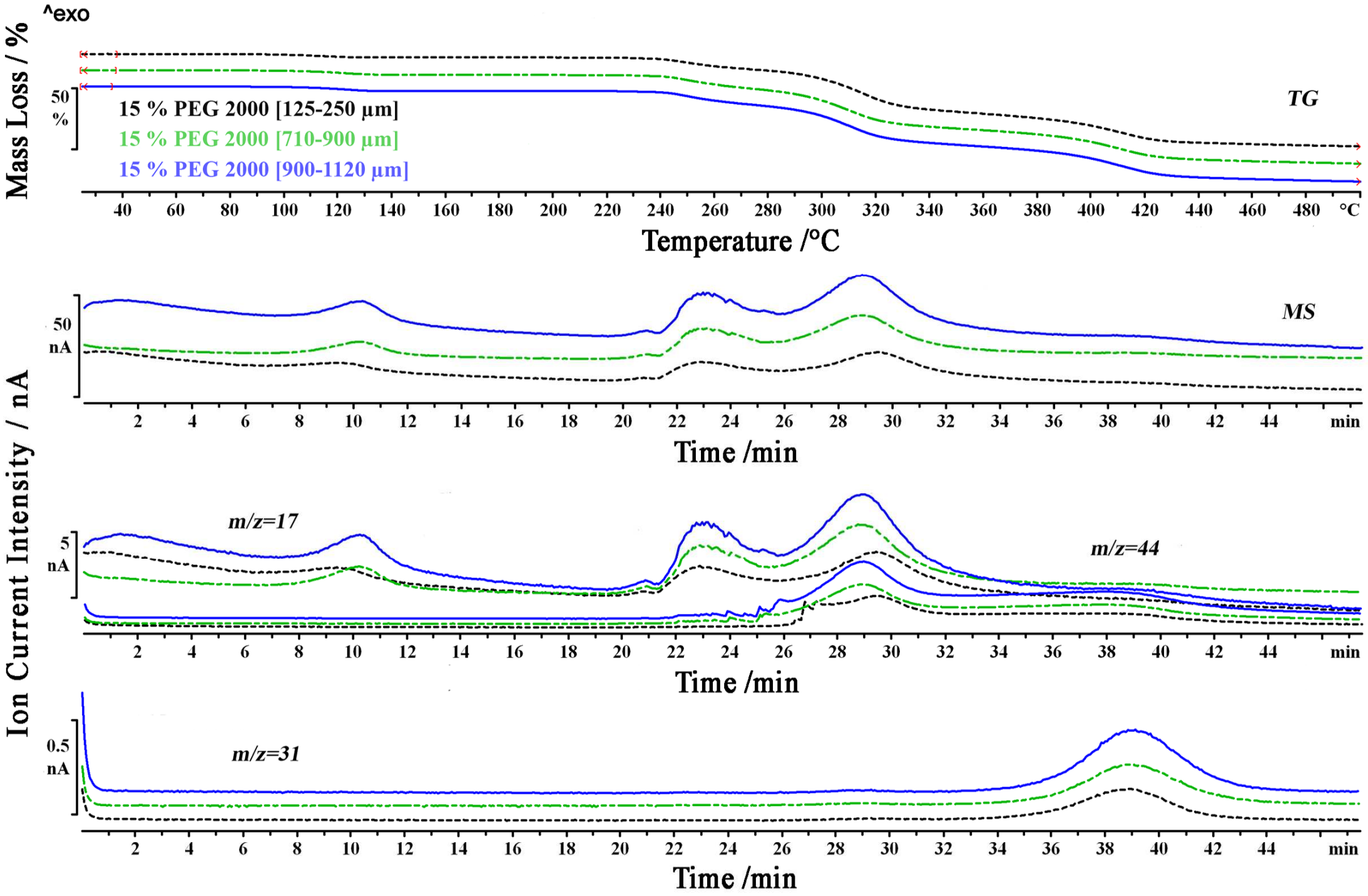
^exo
Mass Loss / %
50 %
15 % PEG 2000 [125-250 µm]
15 % PEG 2000 [710-900 µm]
15 % PEG 2000 [900-1120 µm]
TG
40 60 80 100 120 140 160 180 200 220 240 260 280 300 320 340 360 380 400 420 440 460 480 °C
Temperature /°C
Ion Current Intensity / nA
50 nA
MS
2 4 6 8 10 12 14 16 18 20 22 24 26 28 30 32 34 36 38 40 42 44 min
Time /min
m/z=17
5 nA
m/z=44
2 4 6 8 10 12 14 16 18 20 22 24 26 28 30 32 34 36 38 40 42 44 min
Time /min
0.5 nA
m/z=31
2 4 6 8 10 12 14 16 18 20 22 24 26 28 30 32 34 36 38 40 42 44 min
Time /min

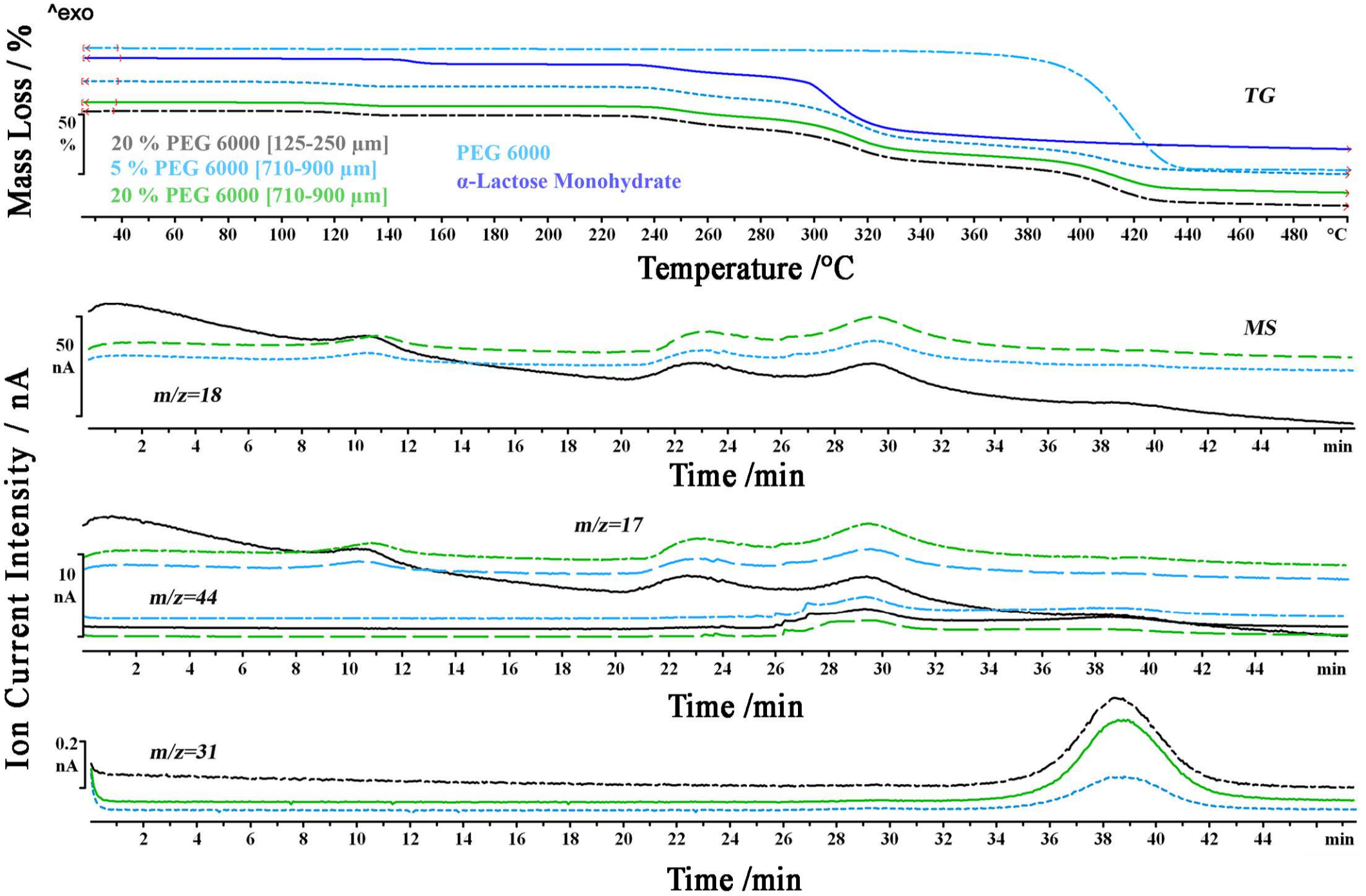
^exo
Mass Loss / %
TG
50
%
20 % PEG 6000 [125-250 µm]
5 % PEG 6000 [710-900 µm]
20 % PEG 6000 [710-900 µm]
PEG 6000
α-Lactose Monohydrate
40 60 80 100 120 140 160 180 200 220 240 260 280 300 320 340 360 380 400 420 440 460 480 °C
Temperature /°C
Ion Current Intensity / nA
MS
50
nA
m/z=18
2 4 6 8 10 12 14 16 18 20 22 24 26 28 30 32 34 36 38 40 42 44 min
Time /min
m/z=17
10
nA
m/z=44
2 4 6 8 10 12 14 16 18 20 22 24 26 28 30 32 34 36 38 40 42 44 min
Time /min
0.2
nA
m/z=31
2 4 6 8 10 12 14 16 18 20 22 24 26 28 30 32 34 36 38 40 42 44 min
Time /min